Molecular Pharmacology Fast Forward. Published on January 2, 2015 as DOI: 10.1124/mol.114.097147
This article has not been copyedited and formatted. The final version may differ from this version.

Title: 1,25-Dihydroxyvitamin D_3 causes ADAM10-dependent ectodomain shedding of TNF receptor 1 in vascular smooth muscle cells.

Won Seok Yang, Hyun Woo Kim, Joo Mi Lee, Nam Jeong Han, Mee Jeong Lee, and Su-Kil Park

Division of Nephrology, Department of Internal Medicine, Asan Medical Center, College of Medicine, University of Ulsan, Seoul, Korea (W.S.Y., S.-K.P.); Division of Nephrology, Department of Internal Medicine, College of Medicine, Jeju National University, Jeju, Korea (H.W.K.); Department of Cell Biology, Asan Institute for Life Sciences, Seoul, Korea (J.M.L., N.J.H.); Department of Pediatrics, College of Medicine, Dankook University, Cheonan, Korea (M.J.L.)

Molecular Pharmacology Fast Forward. Published on January 2, 2015 as DOI: 10.1124/mol.114.097147
This article has not been copyedited and formatted. The final version may differ from this version.

Running title; 1,25-Dihydroxyvitamin D_3 causes TNFR1 shedding.

Corresponding Author; Su-Kil Park, M.D. Department of Internal Medicine, Asan Medical Center, University of Ulsan, 88 Olympic-Ro 43-Gil, SongPa-Gu, Seoul 138-736, Korea. TEL: 82-2-3010-3263, FAX: 82-2-3010-6963, E-mail: skpark@amc.seoul.kr

The number of text pages; 39

The number of tables; 0

The number of figures; 8

The number of references; 44

Abstract; 248 words

Introduction; 475 words

Discussion; 1,379 words

List of Abbreviations;

ADAM, a disintegrin and metalloprotease; AP-1, activator protein-1; 1,25D_3, 1,25-dihydroxyvitamin D_3; DMSO, dimethyl sulfoxide; LOX-1, lectin-like oxidized-low-density lipoprotein receptor-1; NAC, N-acetylcysteine; NF-κB, nuclear factor κB; ODNs, oligodeoxynucleotides; ox-LDL, oxidized low-density lipoprotein; PMA, phorbol 12-myristate 13-acetate; Syk, spleen tyrosine kinase; TNF-α, tumor necrosis factor α; TNFR, tumor necrosis factor receptor; VDR, vitamin D receptor; VSMCs, vascular smooth muscle cells; HASMCs, human aortic smooth muscle cells

Molecular Pharmacology Fast Forward. Published on January 2, 2015 as DOI: 10.1124/mol.114.097147
This article has not been copyedited and formatted. The final version may differ from this version.

Abstract

1,25-Dihydroxyvitamin D_3 ($1,25D_3$) has a potential anti-atherosclerotic effect through anti-inflammatory actions. We investigated how $1,25D_3$ regulates tumor necrosis factor-α (TNF-α)-induced lectin-like oxidized low-density lipoprotein receptor-1 (LOX-1) expression in cultured human aortic smooth muscle cells. TNF-α activated Rac1/reactive oxygen species/spleen tyrosine kinase and transcriptional factors, activator protein-1 and nuclear factor κB, which led to LOX-1 expression. $1,25D_3$ inhibited TNF-α-induced LOX-1 expression by inhibiting Rac1 activation, and thereby its downstream signals. $1,25D_3$ rapidly induced extracellular Ca^{2+} influx. Verapamil, an inhibitor of L-type calcium channels, inhibited $1,25D_3$-induced Ca^{2+} influx and counteracted the inhibitory effects of $1,25D_3$ on Rac1 activation, whereas Bay K8644, an L-type calcium channel agonist, attenuated TNF-α-induced Rac1 activation, as $1,25D_3$ did. $1,25D_3$ induced the ectodomain shedding of TNF receptor 1 (TNFR1), which was abolished by verapamil and in Ca^{2+}-free media. Like $1,25D_3$, Bay K8644 induced the ectodomain shedding of TNFR1. Both $1,25D_3$ and Bay K8644 caused the translocation of a disintegrin and metalloprotease (ADAM) 10 from the cytoplasm to the plasma membrane, which was dependent on extracellular Ca^{2+} influx. In contrast, depletion of ADAM10 by transfection of ADAM10-siRNA prevented $1,25D_3$- or Bay K8644-induced ectodomain shedding of TNFR1 and abolished the suppressive effect of $1,25D_3$ on TNF-α-induced Rac1 activation. Taken together, the findings suggest that $1,25D_3$ induces extracellular Ca^{2+} influx via L-type calcium channel, triggering ADAM10-mediated ectodomain shedding of TNFR1 and, thereby decreases responsiveness to TNF-α. By shedding TNFR1 from the cell surface, $1,25D_3$

Molecular Pharmacology Fast Forward. Published on January 2, 2015 as DOI: 10.1124/mol.114.097147
This article has not been copyedited and formatted. The final version may differ from this version.

may regulate inflammation and atherogenesis, whereas this effect could be attenuated by calcium channel blockers.

Molecular Pharmacology Fast Forward. Published on January 2, 2015 as DOI: 10.1124/mol.114.097147
This article has not been copyedited and formatted. The final version may differ from this version.

Introduction

1,25-Dihydroxyvitamin D_3 ($1,25D_3$) is the active form of vitamin D that regulates calcium and phosphate homeostasis (DeLuca, 2004). In addition to this classical role, $1,25D_3$ has been suggested to have an anti-atherosclerotic effect. In epidemiologic studies, there was a link between vitamin D deficiency and atherosclerotic cardiovascular disease (Dobnig et al., 2008; Giovannucci et al., 2008). In ApoE knockout mice, $1,25D_3$ administration induced a marked reduction in atherosclerotic lesion formation (Takeda et al., 2010; Ish-Shalom et al., 2012). In these studies, $1,25D_3$ was shown to prevent the development of atherosclerosis by changing the function or differentiation of dendritic cells and regulatory T cells (Takeda et al., 2010), or by downregulation of renin-angiotensin system (Ish-Shalom et al., 2012). $1,25D_3$ suppresses renin gene expression by blocking the binding of cAMP response element-binding protein to cAMP response element in the promoter of the gene (Yuan et al., 2007), and thereby reduces the production of angiotensin II, a potent proatherogenic peptide. Beside the suggested mechanisms, the anti-atherosclerotic effect of $1,25D_3$ could be mediated by its anti-inflammatory action.

Atherosclerosis is a chronic inflammatory disease of the arterial wall initiated by lipid overload (Legein et al., 2013). In response to excessive accumulation of atherogenic lipoproteins in the subendothelial space, circulating monocytes are recruited and migrated into the intima and subintima, and transformed into tissue macrophages (Ley et al., 2011). Pro-inflammatory cytokines are released from interactions among the macrophages and the cells comprising the vascular wall, and contribute to the complex cascades of inflammatory processes leading to atherosclerosis (Loppnow et al., 2008).

Lectin-like oxidized-low-density lipoprotein receptor-1 (LOX-1), a receptor for oxidized low-density lipoprotein, is expressed on vascular smooth muscle cells (VSMCs), and participates in the pathogenesis of atherosclerosis (Eto et al., 2006; Kume et al., 2004). Through LOX-1, oxidized low-density lipoprotein stimulates VSMCs to proliferate and migrate into intima, which leads to neointima formation (Eto et al., 2006), and also causes apoptosis of VSMC, leading to plaque instability and rupture (Kume et al., 2004). Pro-inflammatory cytokines including tumor necrosis factor α (TNF-α) stimulate VSMCs to express LOX-1, and thereby may promote the progression of atherosclerotic lesions (Hofnagel et al., 2004).

In a variety of cell types, $1,25D_3$ has been shown to attenuate the effect of TNF-α. $1,25D_3$ inhibited TNF-α-induced nuclear factor κB (NF-κB) activation and expression of E-selectin in human coronary arterial endothelial cells (Suzuki et al., 2009), and also inhibited TNF-α-induced expressions of intercellular adhesion molecule-1 and vascular cell adhesion molecule-1 in human umbilical vein endothelial cells (Martinesi et al., 2006). In fibroblast, $1,25D_3$ suppressed the upregulation of plasminogen activator inhibitor-1 induced by TNF-α (Chen et al., 2011).

Vitamin D receptor is also expressed on VSMCs (Kawashima et al., 1987). In the present study, therefore, we evaluated the effect of $1,25D_3$ on TNF-α-induced LOX-1 expression in human aortic smooth muscle cells (HASMCs), and investigated how $1,25D_3$ regulates the effect of TNF-α.

Molecular Pharmacology Fast Forward. Published on January 2, 2015 as DOI: 10.1124/mol.114.097147
This article has not been copyedited and formatted. The final version may differ from this version.

Materials and Methods

Materials

$1,25D_3$ was obtained from Tocris Bioscience (Bristol, UK). TNF-α was from R&D Systems (Abingdon, UK). BAY 61-3606, Syk inhibitor 574711, (±)-Bay K8644 (Bay K8644) and dimethyl sulfoxide (DMSO) were from EMD Chemicals (Darmstadt, Germany). N-acetylcysteine (NAC), phorbol 12-myristate 13-acetate (PMA), calcium chloride, 4',6-diamidino-2-phenylindole dihydrochloride (DAPI) and probenecid were from Sigma Chemical Co. (St. Louis, MO, USA). NSC 23766 and antibodies to human LOX-1, spleen tyrosine kinase (Syk), a disintegrin and metalloprotease (ADAM) 10 (sc-16524), TNF receptor 1 (TNFR1, sc-8436; raised against amino acids within the extracellular domain of human TNFR1) and actin were from Santa Cruz Biotechnology (Santa Cruz, CA, USA). Antibody to TNF receptor 2 (TNFR2, HP9003; recognizes the extracellular part of human TNFR2) was from Hycult Biotech Inc. (Uden, The Netherlands). Antibody to human phospho-Syk (pY525) was from Epitomics (Burlingame, CA, USA). Rac1-siRNA, ADAM10-siRNA, control-siRNA (Ambion®) and Fluo-4 AM (Molecular probes®) were from Life Technologies (Paisley, UK).

Cell culture

HASMCs were obtained from Lonza Walkersville, Inc. (Walkersville, MD, USA). Cells were cultured in RPMI 1640 (Life Technologies) supplemented with 10% fetal calf serum (Biological Industries Ltd., Cumbernauld, UK). Before each experiment, the cells were rested for 24 h in RPMI 1640 containing 1% fetal calf serum and then refreshed with serum-free RPMI 1640 prior to the addition of various cell signal inhibitors and TNF-α.

Molecular Pharmacology Fast Forward. Published on January 2, 2015 as DOI: 10.1124/mol.114.097147
This article has not been copyedited and formatted. The final version may differ from this version.

Transfection of decoy oligodeoxynucleotides (ODNs) or siRNA

The phosphorothioate double stranded ODNs against the activator protein-1 (AP-1) or NF-κB binding site and the mismatched ODNs were prepared by Bioneer Co. (Daejeon, Korea), as previously (Yang et al., 2010). The sequences of ODNs are as follows : AP-1 decoy ODN, 5'-AGCTTGTGAGTCAGAAGCT-3', mismatched AP-1 decoy ODN, 5'-AGCTTGAATCTCAGAAGCT-3'; NF-κB decoy ODN, 5'-AGTTGAGGGGACTTTCCCAGGC-3', mismatched NF-κB decoy ODN, 5'-AGTTGAGGCGACTTTCCCAGGC-3'. The double stranded ODNs were prepared from complementary single-stranded phosphorothiolate-bonded oligonucleotides. Using Lipofectamine® Reagent (Life Technologies), ODNs or siRNA was transfected to cells seeded in a 6-well plate and cultured for 24 h.

Western blot analysis

Equal amounts of the cell lysates were separated by sodium dodecyl sulfate-polyacrylamide gel electrophoresis and transferred to an Immobilon-P membrane (Millipore, Bedford, MA, USA). The membrane was probed with a primary antibody. Bands were visualized using horseradish peroxidase conjugated secondary antibody and the enhanced chemiluminescence agent (Luminata™ Forte Western HRP Substrate; Millipore).

To detect TNFR1 or TNFR2 in cell culture supernatants, equal amounts of supernatants were precipitated with 20% trichloroacetic acid. After washing with aceteone and air dry, the samples were subjected to immunoblot with anti-TNFR1 or anti-TNFR2 antibody.

Molecular Pharmacology Fast Forward. Published on January 2, 2015 as DOI: 10.1124/mol.114.097147
This article has not been copyedited and formatted. The final version may differ from this version.

Electrophoretic mobility shift assay (EMSA)

Oligonucleotides (Promega, Madison, WI, USA) containing consensus binding-site sequences for AP-1 (5′-CGCTTGATGAGTCAGCCGGAA-3′) and NF-κB (5′ AGTTGAGGGGACTTTCAGGA-3′) were labled by biotin 3' end-labeling kit (Pierce Biotechnology, Rockford, IL, USA). Nuclear extract (5μg) was allowed to react on ice for 15min with biotin-labeled AP-1 or NF-κB oligonucleotides in the buffer containing 12% glycerol; 12mM HEPES, pH7.9; 4mM Tris-HCl, pH7.9; 1mM EDTA; 25mM KCl; 5mM $MgCl_2$; 1μg/ul poly dI-dC (Sigma Chemical Co.). Nucleoprotein–oligonucleotide complexes were resolved by electrophoresis on a 6% polyacrylamide gel at 80 V in 0.5X TBE buffer, and transfered to nylon membrane at 350mA with 0.5X TBE buffer. The blots were UV cross-link at 120mJ/cm^2. DNA–protein complexes were detected using chemiluminescent nucleic acid detection module (Pierce Biotechnology). For the competitive assay, 80 times excess unlabeled AP-1 or NF-κB oligonucleotides were added in the reaction mixture before adding the biotin-labeled AP-1 or NF-κB oligonucleotides.

Pull-down assay for Rac1 activity

Rac1 activation was measured using Active Rac1 Pull-Down and Detection Kit (Pierce Biotechnology), in which glutathione S-transferase-(human p21-activated kinase)-p21 binding domain (GST-Pak1-PBD) fusion protein binds activated Rac1 (Rac1-GTP). Whole cell lysates were incubated with GST-Pak1-PBD fusion protein. The protein-bead complexes were then recovered by centrifugation and washed. Following the last wash, the protein-bead complexes were subjected to Western blot

Molecular Pharmacology Fast Forward. Published on January 2, 2015 as DOI: 10.1124/mol.114.097147
This article has not been copyedited and formatted. The final version may differ from this version.

with a mouse anti-Rac1 antibody. To normalize the protein concentration of each lane, the total amount of Rac1 in whole cell lysates was also determined by Western blot analysis.

Measurement of reactive oxygen species (ROS)

The production of intracellular ROS was evaluated using the probe 5-(and-6)-chloromethyl-2′,7′-dichlorodihydrofluorescein diacetate (CM-H_2DCF-DA; Molecular Probes, Eugene, OR, USA). HASMCs were preincubated with or without NSC 23766, NAC, BAY 61-3606, Syk inhibitor 574711 or 1,25D_3 for 30min and further incubated with TNF-α for 30 min. Five minutes before the end of the incubation period, 5 μM CM-H_2DCF-DA was added to the culture medium. After the incubation, the medium was removed, the cells were washed with phosphate buffered saline (PBS), and intracellular ROS were visualized with a LEICA DM-IRE2 inverted microscope (Leica Microsystem GmbH, Wetzlar, Germany) attached to a Leica TCS-SP2 confocal system (excitation 488 nm, emission 520 nm).

Measurement of intracellular Ca^{2+} by confocal microscopy

HASMCs cultured in a 6-well plate were washed with PBS and loaded with Fluo-4 AM (2 μM) with probenecid (1.5 mM) for 10 min at 37^{o}C in Hank's balanced salt solution (HBSS; Ca^{2+} 1.2 mM). After incubation, the cells were gently washed twice with HBSS, and preincubated with or without verapamil for 2 min and then treated with DMSO (vehicle), 1,25D_3 or Bay K8644. In some experiments, the cells were treated with 1,25D_3 in Ca^{2+}-free HBSS. The Fluo-4 AM in the cells was excited by wavelength at 494 nm and fluorescence images were captured at 506 nm in a 10 sec interval for 5

Molecular Pharmacology Fast Forward. Published on January 2, 2015 as DOI: 10.1124/mol.114.097147
This article has not been copyedited and formatted. The final version may differ from this version.

min using Zeiss LSM710 laser-scanning confocal microscope (Carl Zeiss**,** Germany). The fluorescence intensities were quantified using ZEN 2011 imaging Software (Carl Zeiss, Germany). The change in intracellular Ca^{2+} concentration was represented by relative fluorescence intensity compared with the initial value.

Fluorescence microscopy

To investigate the localization of ADAM10, the cells were washed with PBS, fixed with 4% paraformaldehyde for 10 min, permeabilized with 0.4% Triton X-100 in PBS for 10 min, and incubated with 1% BSA in PBS for 60 min to block nonspecific binding. Thereafter, the cells were incubated with goat anti-ADAM10 antibody overnight at 4 °C, washed 3 times with PBS and then incubated with FITC-conjugated anti-goat IgG secondary antibody. The immunoreactivity for ADAM10 was captured using a confocal microscope.

Statistical Analysis

Data are presented as means ± SE (standard error), with n representing the number of different experiments. An analysis of variance with Dunnett multiple-comparisons test was used to determine statistically significant differences between groups. A p value of <0.05 was considered statistically significant.

Molecular Pharmacology Fast Forward. Published on January 2, 2015 as DOI: 10.1124/mol.114.097147
This article has not been copyedited and formatted. The final version may differ from this version.

Results

$1,25D_3$ inhibits TNF-α-induced LOX-1 expression.

TNF-α stimulated LOX-1 expression. In contrast, $1,25D_3$ significantly attenuated TNF-α-induced LOX-1 expression in a dose-dependent manner, while DMSO, a vehicle for $1,25D_3$, had no effect (Fig. 1).

Involvement of Rac1, ROS, Syk, AP-1 and NF-κB in TNF-α-induced LOX-1 expression.

Rac1, a component of NADPH oxidase, ROS and Syk are known to mediate TNF-α-induced signal transduction in other cell types (Ono et al., 2004; Kim et al., 2012). To test whether Rac1, ROS and Syk are involved in TNF-α-induced LOX-1 expression in HASMCs, the cells were preincubated with or without NSC 23766 (an inhibitor of Rac1), NAC, BAY 61-3606 (an inhibitor of Syk), Syk inhibitor 574711 or DMSO (vehicle) for 30 min, and then stimulated with TNF-α. As shown in Fig. 2A, NSC 23766, NAC, BAY 61-3606 and Syk inhibitor 574711 all significantly attenuated TNF-α-induced LOX-1 expression, while DMSO had no effect.

To assess whether the transcriptional factor AP-1 or NF-κB is implicated in TNF-α-induced LOX-1 expression, the cells were transfected with decoy oligodeoxynucleotides or mismatched oligodeoxynucleotides as a control, and then stimulated with TNF-α. Transfection of AP-1 or NF-κB decoy oligodeoxynucleotides significantly inhibited

Molecular Pharmacology Fast Forward. Published on January 2, 2015 as DOI: 10.1124/mol.114.097147
This article has not been copyedited and formatted. The final version may differ from this version.

TNF-α-induced LOX-1 expression, while mismatched AP-1 or NF-κB decoy oligodeoxynucleotides did not (Fig. 2B).

Sequence of activations of Rac1, ROS, Syk, AP-1 and NF-κB

Because NAC attenuated TNF-α-induced LOX-1 expression, we explored whether TNF-α increases ROS and the relation between ROS and Rac1 or Syk. As shown in Fig. 3A, intracellular ROS were increased by TNF-α. Pretreatment of cells with NSC 23766 or NAC greatly reduced TNF-α-induced ROS accumulation, whereas BAY 61-3606, Syk inhibitor 574711 did not.

Phosphorylation of tyrosines 525 and 526 of human Syk, which are located in the activation loop of the Syk kinase domain, is essential for its function (Zhang et al., 2000). To determine the relation between Syk and Rac1 or ROS, the cells preincubated with/without NSC 23766 or NAC for 30 min were stimulated with TNF-α, and then Syk activation was assessed in the immunoblot of whole cell lysates using an anti-phospho-Syk (pY525) antibody. As shown in Fig. 3B, TNF-α increased Tyr525 phosphorylation of Syk. In contrast, both NSC 23766 and NAC inhibited TNF-α-induced Syk activation. Depletion of Rac1 by transfection of Rac1-siRNA also attenuated TNF-α-induced Syk activation (Fig. 3C).

To evaluate whether Rac1, ROS and Syk are linked to AP-1 or NF-κB activation, the cells were preincubated with/without NSC 23766, NAC, BAY 61-3606, Syk inhibitor 574711 or DMSO for 30 min and then incubated with TNF-α for 15 min. The nuclear fraction was separated and subjected to EMSA. NSC 23766 and NAC markedly

Molecular Pharmacology Fast Forward. Published on January 2, 2015 as DOI: 10.1124/mol.114.097147
This article has not been copyedited and formatted. The final version may differ from this version.

attenuated TNF-α-induced DNA-binding activities of AP-1 and NF-κB (Fig. 3D and 3E). Syk inhibitors, both BAY 61-3606 and Syk inhibitor 574711, markedly attenuated TNF-α-induced DNA-binding activities of AP-1, but not NF-κB (Fig. 3D and 3E).

Next, the cells were incubated with/without TNF-α, and active Rac1 in the whole cell lysates was measured using GST-Pak1-PBD. As shown in Fig. 4A, TNF-α activated Rac1 within 15 min.

$1,25D_3$ inhibits TNF-α-induced Rac1 activation and thereby inhibits its downstream signals.

To determine how $1,25D_3$ attenuates TNF-α-induced LOX-1 expression, we evaluated the effects of $1,25D_3$ on the activations of Rac1, ROS, Syk, AP-1 and NF-κB. As shown in Fig. 4, $1,25D_3$ inhibited TNF-α-induced activations of Rac1 and Syk, and attenuated the increases in ROS and DNA-binding activities of AP-1 and NF-κB.

Inhibitory effect of $1,25D_3$ on TNF-α-induced Rac1 activation is dependent on activation of L-type calcium channels.

$1,25D_3$ activates L-type calcium channels (de Boland and Boland, 1994). We investigated whether activation of L-type calcium channels is involved in $1,25D_3$ inhibition of Rac1 activation. The cells were preincubated with verapamil, $1,25D_3$ or verapamil plus $1,25D_3$ for 30 min, and then stimulated with TNF-α. In the cells preincubated with verapamil plus $1,25D_3$, verapamil was added 2 min prior to $1,25D_3$.

Molecular Pharmacology Fast Forward. Published on January 2, 2015 as DOI: 10.1124/mol.114.097147
This article has not been copyedited and formatted. The final version may differ from this version.

As shown in Fig. 5A, verapamil did not have an effect on TNF-α-induced Rac1 activation, but counteracted the inhibitory effect of $1,25D_3$.

Bay K8644 is an L-type calcium channel agonist (Wahler et al., 1984). To determine whether Bay K8644 has a similar effect, we preincubated the cells with or without Bay K8644 for 30 min, and then stimulated with TNF-α. As shown in Fig. 5B, Bay K8644 also inhibited TNF-α-induced Rac1 activation in a dose-dependent manner.

$1,25D_3$ stimulates extracellular Ca^{2+} influx through L-type calcium channels.

The findings that the effect of $1,25D_3$ was abolished by L-type calcium channel antagonist verapamil, and was mimicked by L-type calcium channel activator Bay K8644 suggest that Ca^{2+} influx may be important in the action of $1,25D_3$. Thus, we tested whether $1,25D_3$ induces Ca^{2+} influx in HASMCs, using Fluo-4 AM, a calcium fluorescent indicator. As shown in Fig. 6, $1,25D_3$ induced a significant increase in the intracellular Ca^{2+} concentration in the presence of extracellular Ca^{2+} (1.2 mM), while DMSO (vehicle) did not. The fluorescent signal intensity reached a maximum rapidly within a minute after $1,25D_3$ addition, and then began to decrease slowly. In contrast, $1,25D_3$-induced increase in intracellular Ca^{2+} was negligible in Ca^{2+}-free media, which indicates that $1,25D_3$ induces an increase in intracellular Ca^{2+} through extracellular Ca^{2+} influx. In addition, $1,25D_3$-induced Ca^{2+} influx was abolished by 2-min preincubation with verapamil. Like $1,25D_3$, Bay K8644 induced a rapid increase in the intracellular Ca^{2+} concentration in the presence of extracellular Ca^{2+} (1.2 mM), while this increase was abolished by preincubation with verapamil.

Molecular Pharmacology Fast Forward. Published on January 2, 2015 as DOI: 10.1124/mol.114.097147
This article has not been copyedited and formatted. The final version may differ from this version.

Extracellular Ca^{2+} influx stimulated by $1,25D_3$ leads to the ectodomain shedding of TNFR1, but not TNFR2.

In a previous study (Porteu et al., 1990), TNF receptors on neutrophil were shedded by calcium ionophore that was used as an agent to activate protein kinase C. Because calcium ionophore allows Ca^{2+} to across the cell membrane and thereby induces extracellular Ca^{2+} influx, we explored whether Ca^{2+} influx through L-type calcium channels causes shedding of TNFR1 or TNFR2 in the cells treated with $1,25D_3$. The cells were incubated with $1,25D_3$, $1,25D_3$ plus verapamil, Bay K8644 or calcium ionophore A23187 for 30 min, and then cell lysates and culture media were analyzed by Western blotting using anti-TNFR1 antibody recognizing the extracellular domain. In the cells treated with verapamil plus $1,25D_3$, verapamil was added 2 min prior to $1,25D_3$. $1,25D_3$ decreased TNFR1 in the cell lysate, and this was accompanied by an increase in the amount of soluble TNFR1 in the medium (Fig. 7A), which was located between 25-kDa and 35-kDa in size, being close to 25-kDa. The changes in TNFR1 by $1,25D_3$ were abrogated by verapamil. Both Bay K8644 and calcium ionophore A23187 also increased the amount of soluble TNFR1 in the medium while decreasing TNFR1 expression in the cells (Fig. 7A).

To determine whether extracellular Ca^{2+} is required for $1,25D_3$-induced ectodomain shedding of TNFR1, we tested the effect of $1,25D_3$ on the cells in Ca^{2+}-free media. As shown in Fig. 7B, $1,25D_3$ failed to induce ectodomain shedding of TNFR1 in the absence of extracellular Ca^{2+}.

Molecular Pharmacology Fast Forward. Published on January 2, 2015 as DOI: 10.1124/mol.114.097147
This article has not been copyedited and formatted. The final version may differ from this version.

RPMI 1640 media, which was used in the present study, contains low Ca^{2+} (0.42 mM) as compared with the physiological level (1.1 - 1.35 mM). To determine the effect of $1,25D_3$ on the cells in physiological extracellular Ca^{2+} concentration, we increased the Ca^{2+} concentration of RPMI 1640 media to 1.2 mM by adding calcium chloride. In this condition, $1,25D_3$ induced TNFR1 shedding at the concentrations of 0.1 - 100 nM, in a dose-dependent manner (Fig. 7C) and more potently than in RPMI 1640 media containing 0.42 mM Ca^{2+}. We also tested the time course of TNFR1 ectodomain shedding of the cells in RPMI 1640 media containing 1.2 mM Ca^{2+}. Most of the ectodomain shedding of TNFR1 occurred within 10 min after treatment with $1,25D_3$ (Fig. 7D).

TNF-α and PMA are known to induce the ectodomain shedding of TNFR2 (Dri et al., 2000; Zhang et al., 2001). In another experiment, the cells were incubated with $1,25D_3$, TNF-α or PMA (the latter two as positive controls), and soluble TNFR2 in the medium and cell lysates was measured by Western blotting using anti-TNFR2 antibody recognizing the extracellular domain. As shown in Fig. 7E, both TNF-α and PMA induced the ectodomain shedding of TNFR2, while $1,25D_3$ did not.

ADAM10 is the sheddase responsible for $1,25D_3$-induced ectodomain shedding of TNFR1

ADAMs, membrane-anchored metalloproteinases, are known to cleave the ectodomains of cell surface receptors (van der Vorst et al., 2012). Because calcium influx is known to activate ADAM10 (Saftig and Reiss, 2011), we investigated the role

Molecular Pharmacology Fast Forward. Published on January 2, 2015 as DOI: 10.1124/mol.114.097147
This article has not been copyedited and formatted. The final version may differ from this version.

of ADAM10 in 1,25D_3-induced TNFR1 ectodomain cleavage. At first, we examined the location of ADAM10 by immunocytochemical staining and confocal microscopy (Fig 8A). ADAM10 was detected predominantly in the cytoplasm of untreated cells. On treatment with 1,25D_3, ADAM10 immunoreactivity increased at the cell surface. In contrast, preincubation with verapamil inhibited 1,25D_3-induced ADAM10 translocation to the cell surface, and 1,25D_3 failed to induce ADAM10 translocation in the absence of extracellular Ca^{2+}. Like 1,25D_3, Bay K8644 also induced ADAM10 translocation to the cell surface in the presence of extracellular Ca^{2+} (1.2 mM), while this translocation was abolished by preincubation with verapamil. In another experiment, we transfected the cells with control-siRNA or ADAM10-siRNA, and treated them with 1,25D_3 or Bay K8644. In Western blot (Fig. 8B-8D), the anti-ADAM10 antibody detected mature ADAM10 (60 kDa), but not the ADAM10 precursor (100 kDa). Depletion of ADAM10 markedly decreased the ectodomain cleavage of TNFR1 induced by either 1,25D_3 (Fig. 8B) or Bay K8644 (Fig. 8C).

We further investigated whether depletion of ADAM10 reverses the inhibitory effect of 1,25D_3 on TNF-α-induced Rac1 activation. As shown in Fig. 8D, 1,25D_3 had little effect on TNF-α-induced Rac1 activation when ADAM10 was depleted.

Molecular Pharmacology Fast Forward. Published on January 2, 2015 as DOI: 10.1124/mol.114.097147
This article has not been copyedited and formatted. The final version may differ from this version.

Discussion

$1,25D_3$ was shown to suppress the effects of TNF-α in many previous studies, but the mechanism has not been clarified. The present study demonstrated that $1,25D_3$ inhibits TNF-α-induced LOX-1 expression in HASMCs, and suggested the mechanism as follows; $1,25D_3$ induces extracellular calcium influx through L-type calcium channel, resulting in translocation of ADAM10 to the plasma membrane, which in turn causes ectodomain shedding of TNFR1 and, thereby decreases responsiveness to TNF-α.

To induce LOX-1 expression in HASMCs, TNF-α activated Rac1 and increased ROS, which in turn activated transcriptional factors AP-1 and NF-κB. NADPH oxidase generates superoxide or H_2O_2. Rac1 is a component of NADPH oxidase and its activation is suggested to stimulate NADPH oxidase activity (Hordijk et al., 2006). In the present study, NSC 23766, a Rac1 inhibitor, abolished the increase in ROS. Syk was also activated and mediated activation of AP-1, but not NF-κB. $1,25D_3$ inhibited activations of all the tested mediators on the signal pathway including Rac1, ROS, Syk, AP-1 and NF-κB. Taken together, the findings suggest that $1,25D_3$ attenuates TNF-α-induced LOX-1 expression by inhibiting activation of Rac1 or earlier steps, and thereby subsequent downstream signals.

$1,25D_3$ interacts with vitamin D receptor and generate genomic responses in the nucleus via either upregulation or downregulation of gene transcription, whereas it also binds to vitamin D receptor in the plasma membrane to generate non-genomic responses (Haussler et al., 2011). Through the latter mode of action, $1,25D_3$ induces rapid activation of L-type calcium channels, causing calcium influx from the extracellular space within a few minutes in osteoblasts and skeletal muscle cells (Uchida et al., 2010;

Molecular Pharmacology Fast Forward. Published on January 2, 2015 as DOI: 10.1124/mol.114.097147
This article has not been copyedited and formatted. The final version may differ from this version.

de Boland and Boland, 1987). The present study also showed that $1,25D_3$ rapidly induces extracellular Ca^{2+} influx through L-type calcium channels in HASMCs; $1,25D_3$ rapidly increased intracellular Ca^{2+}, while this increase was undetectable in the absence of extracellular Ca^{2+}, and $1,25D_3$-induced extracellular Ca^{2+} influx was abolished by the L-type calcium channel antagonist verapamil. The key finding in the present study was that the activation of L-type calcium channels was essential for $1,25D_3$ inhibition of TNF-α-induced Rac1 activation. Verapamil itself did not have an effect on TNF-α-induced Rac1 activation, but completely reversed the inhibitory effect of $1,25D_3$ on TNF-α-induced Rac1 activation. In addition, Bay K8644, an L-type calcium channel agonist, mimicked $1,25D_3$ by inhibiting TNF-α-induced Rac1 activation.

TNF-α exerts its effects by binding to two cell surface receptors, the 55-kDa type 1 (TNFR1) and the 75-kDa type 2 (TNFR2) TNF receptors (Cabal-Hierro and Lazo, 2012). TNFR1 is expressed in almost all cell types, whereas TNFR2 exhibits more restricted expression, being found on lymphoid cells and endothelial cells (Maddahi et al., 2011). VSMCs were shown to express TNFR2 as well as TNFR1 (Maddahi et al., 2011). TNF receptors are transmembrane glycoproteins consisting of extracellular, transmembrane and intracellular regions (Cabal-Hierro and Lazo, 2012). In the present study, $1,25D_3$ caused ectodomain shedding of TNFR1, while it had no effect on TNFR2. Cleavage of TNFR1 leads to the release of soluble TNFR1 (sTNFR1), which not only reduces the number of receptors available on the outside of cells but also causes neutralization of TNF-α in the extracellular space by binding of sTNFR1 to TNF-α, and thereby decreases responsiveness to TNF-α (Wallach et al., 1991). As in Rac1 activation, verapamil reversed $1,25D_3$-induced ectodomain shedding of TNFR1. In the

Molecular Pharmacology Fast Forward. Published on January 2, 2015 as DOI: 10.1124/mol.114.097147
This article has not been copyedited and formatted. The final version may differ from this version.

absence of Ca^{2+} in the culture media, $1,25D_3$ failed to induce ectodomain shedding of TNFR1. In addition, calcium ionophore A23187 as well as Bay K8644 also induced ectodomain shedding of TNFR1. Thus, our findings indicate that $1,25D_3$ causes ectodomain shedding of TNFR1 and it is dependent on extracellular Ca^{2+} influx.

ADAMs are enzymes that cleave the extracellular domains of various cell surface molecules, and there are 12 proteolytically active ADAMs (van der Vorst et al., 2012). ADAM-mediated shedding is induced by different stimuli with activation of different sheddase depending on the stimulus. For an example, both PMA and ionomycin induce ectodomain cleavage of CD44, a type I transmembrane protein functioning as the major cellular adhesion molecule for hyaluronic acid, but the responsible sheddase is different. PMA induces the shedding by activating ADAM17, while ionomycin, an agent causing extracellular calcium influx, induces it by activating ADAM10 (Nagano et al., 2004). So far, ADAMs 17 and 8, but not ADAM10, are known to cleave the extracellular domain of TNFR1 (Bell et al., 2007; Bartsch et al., 2010). In most studies, ADAM17 has been identified as a TNFR1 sheddase, but ADAM8 was responsible for shedding of TNFR1 in the isolated primary neurons and microglia stimulated with TNF-α (Bartsch et al., 2010). Because ADAM17 cleaves TNFR2 as well as TNFR1 (Saftig and Reiss, 2011), shedding of TNFR1, but not TNFR2 by $1,25D_3$ in the present study suggests that ADAM17 is not the responsible sheddase. For the mechanism of ionomycin-induced ADAM10 activation, extracellular calcium influx was suggested to increase the conversion of pro-ADAM10 to the mature form (Nagano et al., 2004), but this was not the case in the present study since both $1,25D_3$ and Bay K8644 did not increase the mature form of ADAM10 in the whole cell lysates. To cleave the ectodomain of TNFR1 at the cell surface, the responsible sheddase should be located in the plasma membrane.

Molecular Pharmacology Fast Forward. Published on January 2, 2015 as DOI: 10.1124/mol.114.097147
This article has not been copyedited and formatted. The final version may differ from this version.

In untreated cells, ADAM10 was detected predominantly in the cytoplasm, but $1,25D_3$ induced ADAM10 translocation to the plasma membrane. This effect was dependent on extracellular Ca^{2+} influx because $1,25D_3$ failed to translocate ADAM10 when the cells were preincubated with verapamil or when Ca^{2+} was absent in the culture media. Consistent with it, the L-type calcium channel agonist Bay K8644 also increased ADAM10 translocation to the plasma membrane while this effect was inhibited by verapamil. Our study also showed that depletion of ADAM10 by transfection of ADAM10-siRNA prevented $1,25D_3$-induced ectodomain shedding of TNFR1 and abolished the suppressive effect of $1,25D_3$ on TNF-α-induced Rac1 activation. Bay K8644-induced ectodomain shedding of TNFR1 was also prevented by the depletion of ADAM10. Based on the findings, it was considered that $1,25D_3$ causes extracellular Ca^{2+} influx, which triggers translocation of ADAM10 to the plasma membrane, which in turn makes it possible to cleave the ectodomain of TNFR1 at the cell surface.

The driving force for calcium influx induced by $1,25D_3$ may depend on the concentration gradient between extracellular and intracellular calciums. Normally, extracellular concentrations of calcium are in the range of 2.2-2.6 mM. About 50 per cent of the total calcium in the plasma exists in the ionized form (1.10-1.35 mM) (Peacock, 2010). Compared with extracellular calcium, intracellular calcium concentrations are much low (about 100 nM in the resting state) (Guerini et al., 2005). This large concentration gradient across the cell membrane is formed by various plasma membrane calcium pumps and Na^{+}/Ca^{++} exchanger. In the present study, the ectodomain shedding of TNFR1 induced by $1,25D_3$ was dose-dependent and was significant at the concentration as low as 100 pM when calcium concentration in the culture media was adjusted to 1.2 mM.

Molecular Pharmacology Fast Forward. Published on January 2, 2015 as DOI: 10.1124/mol.114.097147
This article has not been copyedited and formatted. The final version may differ from this version.

TNF-α is crucially involved in the pathogenesis and progression of atherosclerosis by altering endothelial and vascular smooth muscle cell function (Kleinbongard et al., 2010). It induces the expression of LOX-1 in vascular smooth muscle cells as well as endothelial cells (Kume et al., 1998; DeLuca, 2004; Hofnagel et al., 2004). In animal models, overexpression of LOX-1 accelerated intramyocardial vasculopathy and the atheroma-like lesion (Inoue et al., 2005), whereas deletion of LOX-1 reduced atherogenesis (Mehta et al., 2007). Thus, LOX-1 is considered to be a possible therapeutic target for the treatment of atherosclerotic diseases (Xu et al., 2013). The present study shows that $1,25D_3$ inhibits TNF-α-induced LOX-1 expression on HASMCs. In view of the mechanism of inhibition revealed in the present study, however, $1,25D_3$ is likely to attenuate the overall effects of TNF-α rather than inhibits specifically the expression of LOX-1. Calcium channel blockers are commonly used for arrhythmia or hypertension. Because $1,25D_3$-induced ectodomain shedding of TNFR1 was dependent on extracellular Ca^{2+} influx through L-type calcium channels, our data also suggest that calcium channel blockers may interfere with the anti-inflammatory and anti-atherosclerotic actions of $1,25D_3$, but this possibility needs to be further investigated in the animal or human studies.

In summary, $1,25D_3$ causes ADAM10-mediated ectodomain shedding of TNFR1 in HASMCs. By shedding TNFR1 from the cell surface, $1,25D_3$ may participate in the regulation of inflammation and atherogenesis, whereas this effect could be attenuated by calcium channel blockers.

Molecular Pharmacology Fast Forward. Published on January 2, 2015 as DOI: 10.1124/mol.114.097147
This article has not been copyedited and formatted. The final version may differ from this version.

Acknowledgment

We thank Kim Jin Ju and Moon Soo Young for excellent technical assistance.

Molecular Pharmacology Fast Forward. Published on January 2, 2015 as DOI: 10.1124/mol.114.097147
This article has not been copyedited and formatted. The final version may differ from this version.

Authorship Contributions

Participated in research design: Yang, Park

Conducted experiments: J.M.Lee, Han, Kim

Performed data analysis: Yang, Park, M.J.Lee

Wrote or contributed to the writing of the manuscript: Yang, Kim, M.J.Lee, Park

Molecular Pharmacology Fast Forward. Published on January 2, 2015 as DOI: 10.1124/mol.114.097147
This article has not been copyedited and formatted. The final version may differ from this version.

References

Bartsch JW, Wildeboer D, Koller G, Naus S, Rittger A, Moss ML, Minai Y, Jockusch H (2010) Tumor necrosis factor-α (TNF-α) regulates shedding of TNF-α receptor 1 by the metalloprotease-disintegrin ADAM8: evidence for a protease-regulated feedback loop in neuroprotection. *J Neurosci* **30**:12210-12218.

Bell JH, Herrera AH, Li Y, Walcheck B (2007) Role of ADAM17 in the ectodomain shedding of TNF-α and its receptors by neutrophils and macrophages. *J Leukoc Biol* **82**:173-176.

Cabal-Hierro L, Lazo PS (2012) Signal transduction by tumor necrosis factor receptors. *Cell Signal* **24**:1297-1305.

Chen Y, Kong J, Sun T, Li G, Szeto FL, Liu W, Deb DK, Wang Y, Zhao Q, Thadhani R, Li YC (2011) 1,25-Dihydroxyvitamin D_3 suppresses inflammation-induced expression of plasminogen activator inhibitor-1 by blocking nuclear factor-κB activation. Arch Biochem Biophys **507**:241-247.

de Boland AR, Boland RL (1987) Rapid changes in skeletal muscle calcium uptake induced in vitro by 1,25-dihydroxyvitamin D3 are suppressed by calcium channel blockers. Endocrinology **120**:1858-1864.

de Boland AR, Boland RL (1994) Non-genomic signal transduction pathway of vitamin D in muscle. Cell Signal **6**:717-724.

DeLuca HF (2004). Overview of general physiologic features and functions of vitamin D. *Am J Clin Nutr* **80**:1689S-1696S.

Dobnig H, Pilz S, Scharnagl H, Renner W, Seelhorst U, Wellnitz B, Kinkeldei J, Boehm BO, Weihrauch G, Maerz W (2008) Independent association of low serum 25-hydroxyvitamin D and 1,25-dihydroxyvitamin D levels with all-cause and cardiovascular mortality. *Arch Intern Med* **168**:1340-1349.

Dri P, Gasparini C, Menegazzi R, Cramer R, Albéri L, Presani G, Garbisa S, Patriarca P (2000) TNF-Induced shedding of TNF receptors in human polymorphonuclear leukocytes: role of the 55-kDa TNF receptor and involvement of a membrane-bound and non-matrix metalloproteinase. *J Immunol* **165**:2165-2172.

Eto H, Miyata M, Kume N, Minami M, Itabe H, Orihara K, Hamasaki S, Biro S, Otsuji Y, Kita T, Tei C (2006) Expression of lectin-like oxidized LDL receptor-1 in smooth muscle cells after vascular injury. *Biochem Biophys Res Commun* **341**:591-598.

Giovannucci E, Liu Y, Hollis BW, Rimm EB (2008) 25-hydroxyvitamin D and risk of myocardial infarction in men: a prospective study. *Arch Intern Med* **168**:1174-1180.

Guerini D, Coletto L, Carafoli E (2005) Exporting calcium from cells. *Cell Calcium* **38**:281-289.

Haussler MR, Jurutka PW, Mizwicki M, Norman AW (2011) Vitamin D receptor (VDR)-mediated actions of 1α,25(OH)₂vitamin D₃: genomic and non-genomic mechanisms. *Best Pract Res Clin Endocrinol Metab* **25**:543-559.

Hofnagel O, Luechtenborg B, Stolle K, Lorkowski S, Eschert H, Plenz G, Robenek H (2004) Proinflammatory cytokines regulate LOX-1 expression in vascular smooth muscle cells. *Arterioscler Thromb Vasc Biol* **24**:1789-1795.

Hordijk PL (2006) Regulation of NADPH oxidases: the role of Rac proteins. *Circ Res* **98**:453-462.

Inoue K, Arai Y, Kurihara H, Kita T, Sawamura T (2005) Overexpression of lectin-like oxidized low-density lipoprotein receptor-1 induces intramyocardial vasculopathy in apolipoprotein E-null mice. *Circ Res* **97**:176-184.

Ish-Shalom M, Sack J, Vechoropoulos M, Shaish A, Entin-Meer M, Kamari Y, Maysel-Auslender S, Keren G, Harats D, Stern N, Tordjman K (2012) Low-dose calcitriol decreases aortic renin, blood pressure, and atherosclerosis in apoe-null mice. *J Atheroscler Thromb* **19**:422-434.

Kawashima H (1987) Receptor for 1,25-dihydroxyvitamin D in a vascular smooth muscle cell line derived from rat aorta. *Biochem Biophys Res Commun* **146**:1-6.

Kim YJ, Koo TY, Yang WS, Han NJ, Jeong JU, Lee SK, Park SK (2012) Activation of spleen tyrosine kinase is required for TNF-α-induced endothelin-1 upregulation in human aortic endothelial cells. *FEBS Lett* **586**:818-826.

Kleinbongard P, Heusch G, Schulz R (2010) TNFα in atherosclerosis, myocardial ischemia/reperfusion and heart failure. *Pharmacol Ther* **127**:295-314.

Kume N, Murase T, Moriwaki H, Aoyama T, Sawamura T, Masaki T, Kita T (1998) Inducible expression of lectin-like oxidized LDL receptor-1 in vascular endothelial cells. *Circ Res* **83**:322-327.

Kume N, Kita T (2004) Apoptosis of vascular cells by oxidized LDL: involvement of caspases and LOX-1 and its implication in atherosclerotic plaque rupture. *Circ Res* **94**:269-270.

Legein B, Temmerman L, Biessen EA, Lutgens E (2013) Inflammation and immune system interactions in atherosclerosis. *Cell Mol Life Sci* **70**:3847-3869.

Ley K, Miller YI, Hedrick CC (2011) Monocyte and macrophage dynamics during atherogenesis. *Arterioscler Thromb Vasc Biol* **31**:1506-1516.

Loppnow H, Werdan K, Buerke M (2008) Vascular cells contribute to atherosclerosis by cytokine- and innate-immunity-related inflammatory mechanisms. *Innate Immun* **14**:63-87.

Maddahi A, Kruse LS, Chen QW, Edvinsson L (2011) The role of tumor necrosis factor-α and TNF-α receptors in cerebral arteries following cerebral ischemia in rat. *J Neuroinflammation* **8**:107.

Martinesi M, Bruni S, Stio M, Treves C (2006) 1,25-Dihydroxyvitamin D_3 inhibits tumor necrosis factor-α-induced adhesion molecule expression in endothelial cells. *Cell Biol Int* **30**:365-375.

Mehta JL, Sanada N, Hu CP, Chen J, Dandapat A, Sugawara F, Satoh H, Inoue K, Kawase Y, Jishage K, Suzuki H, Takeya M, Schnackenberg L, Beger R, Hermonat PL, Thomas M, Sawamura T (2007) Deletion of LOX-1 reduces atherogenesis in LDLR knockout mice fed high cholesterol diet. *Circ Res* **100**:1634-1642.

Nagano O, Murakami D, Hartmann D, De Strooper B, Saftig P, Iwatsubo T, Nakajima M, Shinohara M, Saya H (2004) Cell-matrix interaction via CD44 is independently regulated by different metalloproteinases activated in response to extracellular Ca^{2+} influx and PKC activation. *J Cell Biol* **165**:893-902.

Ono H, Ichiki T, Fukuyama K, Iino N, Masuda S, Egashira K, Takeshita A (2004) cAMP-response element-binding protein mediates tumor necrosis factor-α-induced vascular smooth muscle cell migration. *Arterioscler Thromb Vasc Biol* **24**:1634-1639.

Peacock M (2010) Calcium metabolism in health and disease. *Clin J Am Soc Nephrol* **5**:S23-30.

Porteu F, Nathan C (1990) Shedding of tumor necrosis factor receptors by activated human neutrophils. *J Exp Med* **172**:599-607.

Saftig P, Reiss K (2011) The "A Disintegrin And Metalloproteases" ADAM10 and ADAM17: novel drug targets with therapeutic potential? *Eur J Cell Biol* **90**:527-535.

Suzuki Y, Ichiyama T, Ohsaki A, Hasegawa S, Shiraishi M, Furukawa S (2009) Anti-inflammatory effect of 1α,25-dihydroxyvitamin D_3 in human coronary arterial endothelial cells: Implication for the treatment of Kawasaki disease. *J Steroid Biochem Mol Biol* **113**:134-138.

Takeda M, Yamashita T, Sasaki N, Nakajima K, Kita T, Shinohara M, Ishida T, Hirata K (2010) Oral administration of an active form of vitamin D_3 (calcitriol) decreases atherosclerosis in mice by inducing regulatory T cells and immature dendritic cells with tolerogenic functions. *Arterioscler Thromb Vasc Biol* **30**:2495-2503.

Uchida Y, Endoh T, Shibukawa Y, Tazaki M, Sueishi K (2010) 1α,25-dihydroxyvitamin D_3 rapidly modulates Ca^{2+} influx in osteoblasts mediated by Ca^{2+} channels. *Bull Tokyo Dent Coll* **51**:221-226.

van der Vorst EP, Keijbeck AA, de Winther MP, Donners MM (2012) A disintegrin and metalloproteases: molecular scissors in angiogenesis, inflammation and atherosclerosis. *Atherosclerosis* **224**:302-308.

Wahler GM, Sperelakis N (1984) New Ca^{2+} agonist (Bay K 8644) enhances and induces cardiac slow action potentials. *Am J Physiol* **247**:H337-340.

Wallach D, Engelmann H, Nophar Y, Aderka D, Kemper O, Hornik V, Holtmann H, Brakebusch C (1991) Soluble and cell surface receptors for tumor necrosis factor. *Agents Actions Suppl* **35**:51-57.

Xu S, Ogura S, Chen J, Little PJ, Moss J, Liu P (2013) LOX-1 in atherosclerosis: biological functions and pharmacological modifiers. *Cell Mol Life Sci* **70**:2859-2872.

Yang WS, Lee JM, Han NJ, Kim YJ, Chang JW, Park SK (2010) Mycophenolic acid attenuates tumor necrosis factor-α-induced endothelin-1 production in human aortic endothelial cells. *Atherosclerosis* **211**:48-54.

Yuan W, Pan W, Kong J, Zheng W, Szeto FL, Wong KE, Cohen R, Klopot A, Zhang Z, Li YC (2007) 1,25-dihydroxyvitamin D_3 suppresses renin gene transcription by blocking the activity of the cyclic AMP response element in the renin gene promoter. *J Biol Chem* **282**:29821-29830.

Zhang J, Billingsley ML, Kincaid RL, Siraganian RP (2000) Phosphorylation of Syk activation loop tyrosines is essential for Syk function. An in vivo study using a specific anti-Syk activation loop phosphotyrosine antibody. *J Biol Chem* **275**:35442-35447.

Zhang Z, Oliver P, Lancaster JR Jr, Schwarzenberger PO, Joshi MS, Cork J, Kolls JK (2001) Reactive oxygen species mediate tumor necrosis factor alpha-converting, enzyme-dependent ectodomain shedding induced by phorbol myristate acetate. *FASEB J* **15**:303-305.

Molecular Pharmacology Fast Forward. Published on January 2, 2015 as DOI: 10.1124/mol.114.097147
This article has not been copyedited and formatted. The final version may differ from this version.

Footnote to the title

This work was supported by the Asan Institute for Life Sciences (Seoul, Korea) [Grant 02-200].

Molecular Pharmacology Fast Forward. Published on January 2, 2015 as DOI: 10.1124/mol.114.097147
This article has not been copyedited and formatted. The final version may differ from this version.

Figure legends

Fig. 1. $1,25D_3$ inhibits TNF-α-induced LOX-1 expression. HASMCs were preincubated with different concentrations of $1,25D_3$ or DMSO (vehicle) for 30 min, and then stimulated with TNF-α (10 ng/ml) for 24 h. Whole cell lysates were immunoblotted with an anti-LOX-1 antibody. (n=3, *$p < 0.05$ compared with control; **$p < 0.05$ as compared with TNF-α).

Fig. 2. Involvement of Rac1, ROS, Syk, AP-1 and NF-κB in TNF-α-induced LOX-1 expression. (A) HASMCs were preincubated with NSC 23766 (50 μM), NAC (5 mM), BAY 61-3606 (1 μM), Syk inhibitor 574711 (1 μM) or DMSO (vehicle) for 30 min, and then stimulated with TNF-α (10 ng/ml) for 24 h. (B) HASMCs transfected with AP-1 or NF-κB decoy oligodeoxynucleotides, or mismatched oligodeoxynucleotides were incubated with TNF-α (10 ng/ml) for 24 h. Whole cell lysates were immunoblotted with an anti-LOX-1 antibody. (n=3, *$p < 0.05$ compared with control; **$p < 0.05$ as compared with TNF-α).

Fig. 3. Sequence of activations of Rac1, ROS, Syk, AP-1 and NF-κB. (A) Rac1 and Syk in ROS generation. HASMCs preincubated with NSC 23766 (50 μM), NAC (5 mM), BAY 61-3606 (1 μM) or Syk inhibitor 574711 (1 μM) for 30 min were incubated with TNF-α (10 ng/ml) for 30 min. Intracellular ROS reacted with CM-H_2DCF-DA was visualized with confocal microscopy (×200). The result shown is representative of three independent experiments. (B,C) Rac1 and ROS precede Syk activation. HASMCs

Molecular Pharmacology Fast Forward. Published on January 2, 2015 as DOI: 10.1124/mol.114.097147
This article has not been copyedited and formatted. The final version may differ from this version.

preincubated with NSC 23766 or NAC were stimulated with TNF-α for 30 min (B). HASMCs transfected with control-siRNA or Rac1-siRNA were stimulated with TNF-α for 30 min (C). Whole-cell lysates were immunoblotted with an anti-phospho-Syk antibody. (n=4, *p < 0.05 compared with control; **p < 0.05 as compared with TNF-α). (D,E) Rac1, ROS and Syk regulate AP-1 and NF-κB activation. HASMCs preincubated with NSC 23766, NAC, BAY 61-3606, Syk inhibitor 574711 or DMSO were stimulated with TNF-α for 30 min. The nuclear extracts were assayed for the ability to bind biotin-labeled AP-1 (D) or NF-κB (E) oligonucleotides by electrophoretic mobility shift assay. The results shown are representative of three independent experiments.

Fig. 4. 1,25D_3 inhibits TNF-α-induced Rac1, ROS, Syk activation and AP-1 and NF-κB DNA binding activities. (A) HASMCs were preincubated with 1,25D_3 (120 nM) for 30 min, and then stimulated with TNF-α (10 ng/ml) for 15 min. Active Rac1 (Rac1-GTP) in whole-cell lysate was precipitated using GST-Pak1-PBD beads and analyzed by Western blotting. Total Rac1 in whole-cell lysate was also analyzed. (n=4, *p < 0.05 compared with control; **p < 0.05 as compared with TNF-α). (B) HASMCs preincubated with 1,25D_3 for 30 min, and then stimulated with TNF-α for 30 min. Intracellular ROS reacted with CM-H_2DCF-DA was visualized with confocal microscopy (×200). The result shown is representative of three independent experiments. (C) HASMCs preincubated with 1,25D_3 for 30 min, and then stimulated with TNF-α for 30 min. Whole-cell lysates were immunoblotted with an anti-phospho-Syk antibody. (n=4, *p < 0.05 compared with control; **p < 0.05 as compared with TNF-α). (D,E) HASMCs preincubated with 1,25D_3 (120 nM) were stimulated with

Molecular Pharmacology Fast Forward. Published on January 2, 2015 as DOI: 10.1124/mol.114.097147
This article has not been copyedited and formatted. The final version may differ from this version.

TNF-α. The nuclear extracts were assayed for the ability to bind biotin-labeled AP-1 (D) or NF-κB (E) oligonucleotides by electrophoretic mobility shift assay. The results shown are representative of three independent experiments.

Fig. 5. Inhibitory effect of $1,25D_3$ on TNF-α-induced Rac1 activation is dependent on activation of L-type calcium channels. (A) Verapamil counteracts the inhibitory effect of $1,25D_3$ on TNF-α-induced Rac1 activation. HASMCs were preincubated with verapamil (1 μM), $1,25D_3$ (120 nM) or verapamil (1 μM) plus $1,25D_3$ (120 nM) for 30 min, and then stimulated with TNF-α (10 ng/ml) for 15 min. In the cells preincubated with verapamil plus $1,25D_3$, verapamil was added 2 min prior to $1,25D_3$. (B) Bay K8644 inhibits TNF-α-induced Rac1 activation. HASMCs were preincubated with different concentrations of Bay K8644 for 30 min, and then stimulated with TNF-α (10 ng/ml) for 15 min. Active Rac1 in whole-cell lysate was precipitated using GST-Pak1-PBD beads and analyzed by Western blotting. Total Rac1 in whole-cell lysate was also analyzed. A representative blot from one of three independent experiments is shown. The bar graph shows the relative densities of Rac1-GTP/total Rac1 bands (n=3, *$p < 0.05$ compared with control; **$p < 0.05$ as compared with TNF-α).

Fig. 6. $1,25D_3$ induces extracellular Ca^{2+}-influx through L-type calcium channel. HASMCs were loaded with Fluo-4 AM (2 μM), then treated with DMSO (vehicle), $1,25D_3$ (100 nM) or Bay K8644 (1 μM) with or without 2-min preincubation with verapamil (1 μM). The experiments were performed on the cells in HBSS containing 1.2 mM Ca^{2+} or HBSS free of Ca^{2+}. Additions of DMSO, $1,25D_3$ and Bay K8644 are

indicated by arrows. (A) Representative images before and after treatment. (B) Time-response traces of intracellular Ca^{2+} fluorescence intensity. (means ± SE of n = 47 - 63 cells in each group from three independent experiments)

Fig. 7. $1,25D_3$ induces the ectodomain shedding of TNFR1, but not TNFR2; the TNFR1 shedding is dependent on extracelluar Ca^{2+} influx. (A) HASMCs in RPMI 1640 media (calcium 0.42 mM) were incubated with $1,25D_3$, verapamil (1 μM) plus $1,25D_3$, Bay K8644 (1 μM) or calcium ionophore A23187 (2 μM) for 30 min. (n=3) In the cells incubated with verapamil plus $1,25D_3$, verapamil was added 2 min prior to $1,25D_3$. (B) HASMCs were incubated with $1,25D_3$ (100 nM) for 30 min in DMEM media containing 1.2 mM Ca^{2+} or DMEM media free of Ca^{2+}. (n=5) (C,D) HASMCs in calcium-supplemented RPMI 1640 media (Ca^{2+} 1.2 mM) were incubated with different concentrations of $1,25D_3$ for 30 min, or $1,25D_3$ (100 nM) for different times. (n=3) (E) HASMCs in RPMI 1640 media (calcium 0.42 mM) were incubated with $1,25D_3$, TNF-α (10 ng/ml), or PMA (20 ng/ml) for 30 min. (n=3) Culture media and cell lysates were analyzed by Western blotting using anti-TNFR1 (A-D) or TNFR2 antibody (E). *$p < 0.05$ compared with control; **$p < 0.05$ as compared with $1,25D_3$ (240 nM)).

Fig. 8. ADAM10 is the sheddase responsible for $1,25D_3$-induced ectodomain shedding of TNFR1.

(A) $1,25D_3$ induces extracellular Ca^{2+} influx-dependent ADAM10 translocation from the cytoplasm to the plasma membrane. HASMCs in 1.2 mM Ca^{2+} containing media were incubated for 10 min with DMSO (vehicle), $1,25D_3$ (100 nM) or Bay K8644 (1 μM) with or without 2-min preincubation with verapamil (1 μM). In another well, the

Molecular Pharmacology Fast Forward. Published on January 2, 2015 as DOI: 10.1124/mol.114.097147
This article has not been copyedited and formatted. The final version may differ from this version.

cells in Ca^{2+}-free media were also incubated for 10 min with 1,25D_3 (100 nM). After then, the cells were permeabilized with Triton-X and immunostained for ADAM10, and visualized with confocal microscopy. Cell nuclei were stained with DAPI. Representative images from three independent experiments with similar results are shown. Note that ADAM10 immunoreactivity at the surface of the cells treated with 1,25D_3 or Bay K8644 in the presence of extracellular Ca^{2+} (1.2 mM). (B,C) Depletion of ADAM10 abolishes 1,25D_3- or Bay K8644-induced ectodomain shedding of TNFR1. HASMCs were transfected with control-siRNA or ADAM10-siRNA, and then incubated with 1,25D_3 (120 nM) (B) or Bay K8644 (1 μM) (C) for 30 min. Culture media and cell lysates were analyzed by Western blotting using anti-TNFR1 antibody. (n=3, *$p < 0.05$ compared with control). (D) Depletion of ADAM10 abolishes the inhibitory effect of 1,25D_3 on TNF-α-induced Rac1 activation. HASMCs were transfected with control-siRNA or ADAM10-siRNA, and then were preincubated with or without 1,25D_3 (120 nM) for 30 min, and then stimulated with TNF-α (10 ng/ml) for 15 min. Active Rac1 (Rac1-GTP) in whole-cell lysate was precipitated using GST-Pak1-PBD beads and analyzed by Western blotting. Total Rac1 in whole-cell lysate was also analyzed. (n=3, *$p < 0.05$ compared with control).

Figure 1

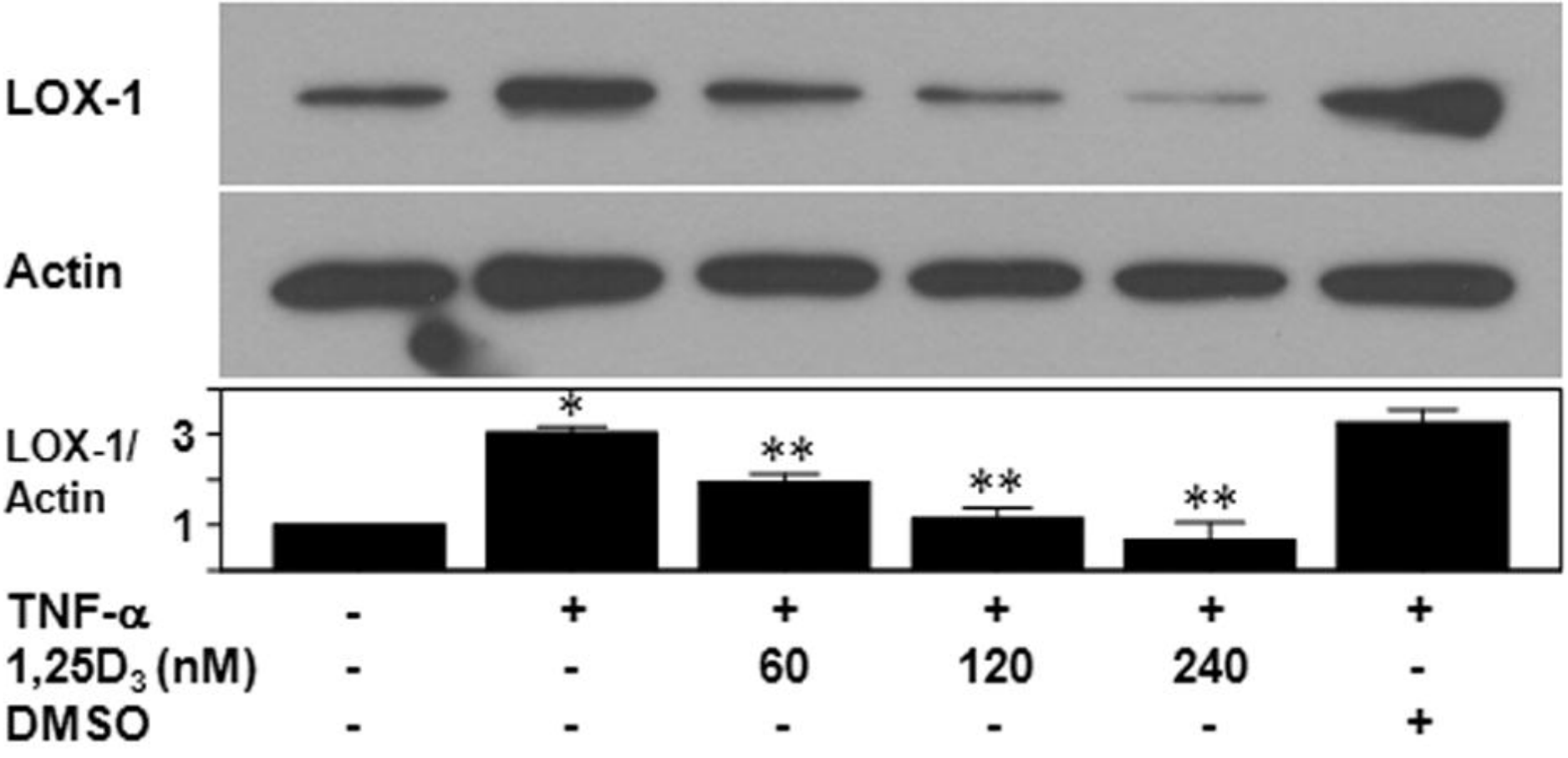

Figure 2

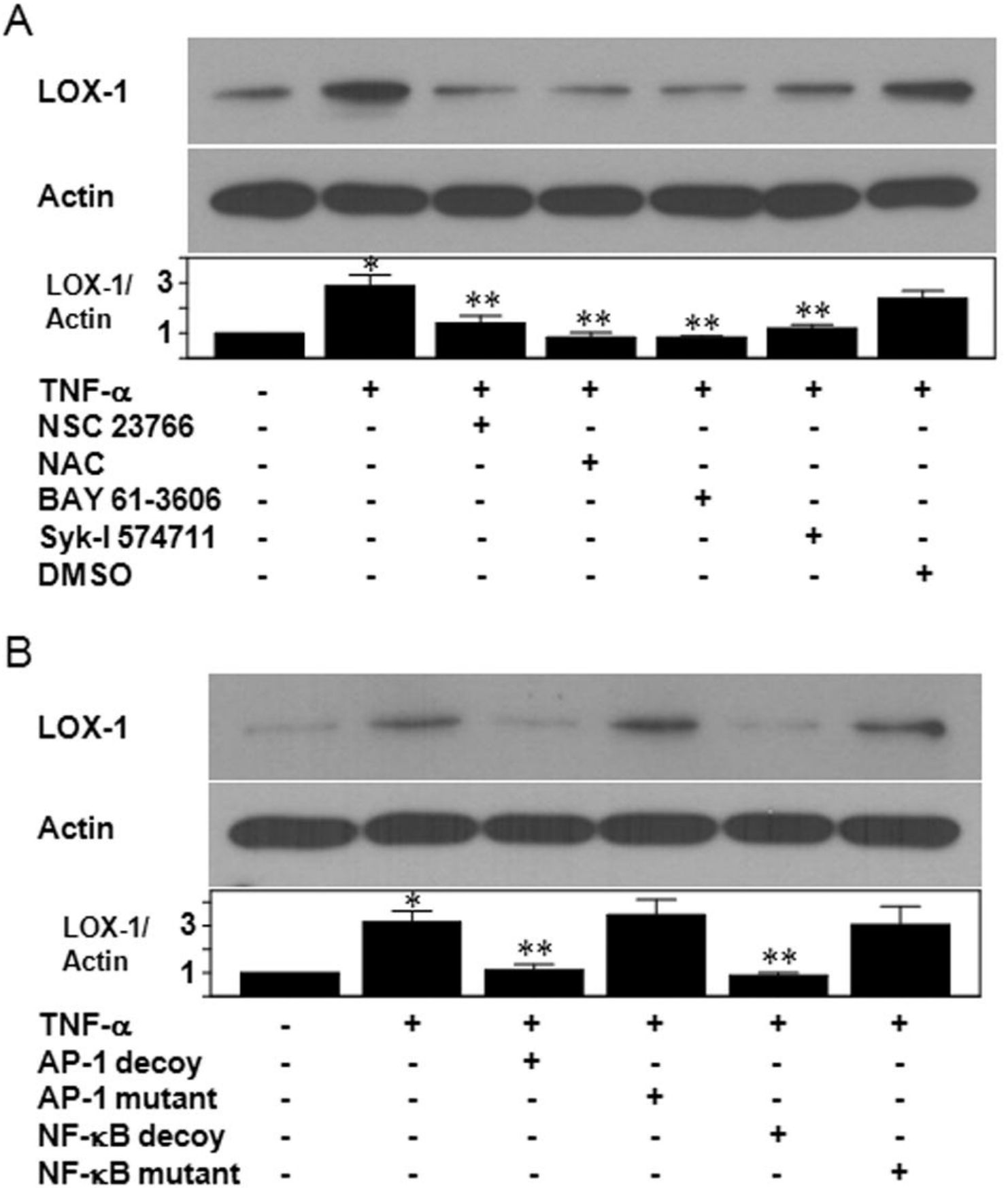
A
LOX-1
Actin
LOX-1/ Actin
3
1
*
**
**
**
**
TNF-α - + + + + + +
NSC 23766 - - + - - - -
NAC - - - + - - -
BAY 61-3606 - - - - + - -
Syk-I 574711 - - - - - + -
DMSO - - - - - - +
B
LOX-1
Actin
LOX-1/ Actin
3
1
*
**
**
TNF-α - + + + + +
AP-1 decoy - - + - - -
AP-1 mutant - - - + - -
NF-κB decoy - - - - + -
NF-κB mutant - - - - - +

Figure 3

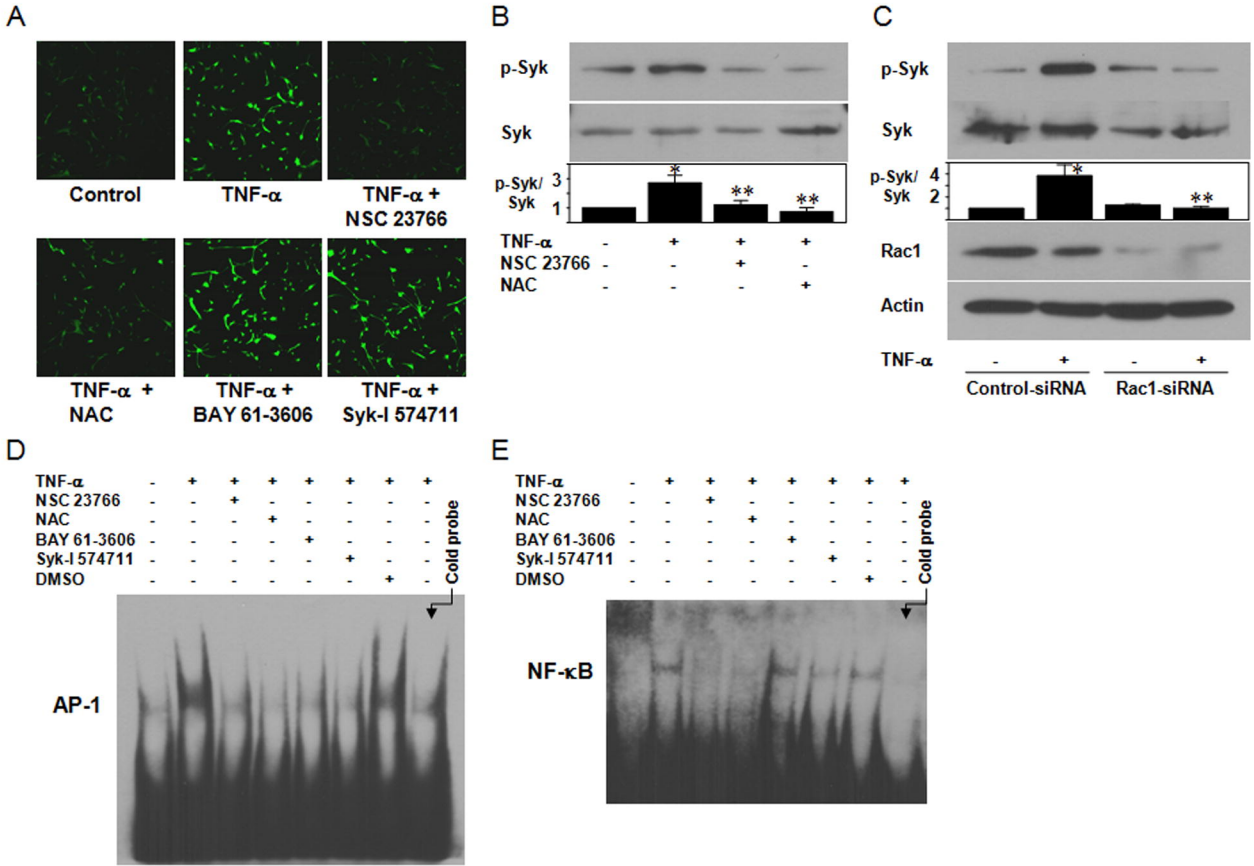
A
Control
TNF-α
TNF-α + NSC 23766
TNF-α + NAC
TNF-α + BAY 61-3606
TNF-α + Syk-I 574711
B
p-Syk
Syk
p-Syk/ Syk
TNF-α
NSC 23766
NAC
C
p-Syk
Syk
p-Syk/ Syk
Rac1
Actin
TNF-α
Control-siRNA
Rac1-siRNA
D
TNF-α
NSC 23766
NAC
BAY 61-3606
Syk-I 574711
DMSO
Cold probe
AP-1
E
TNF-α
NSC 23766
NAC
BAY 61-3606
Syk-I 574711
DMSO
Cold probe
NF-κB

Figure 4

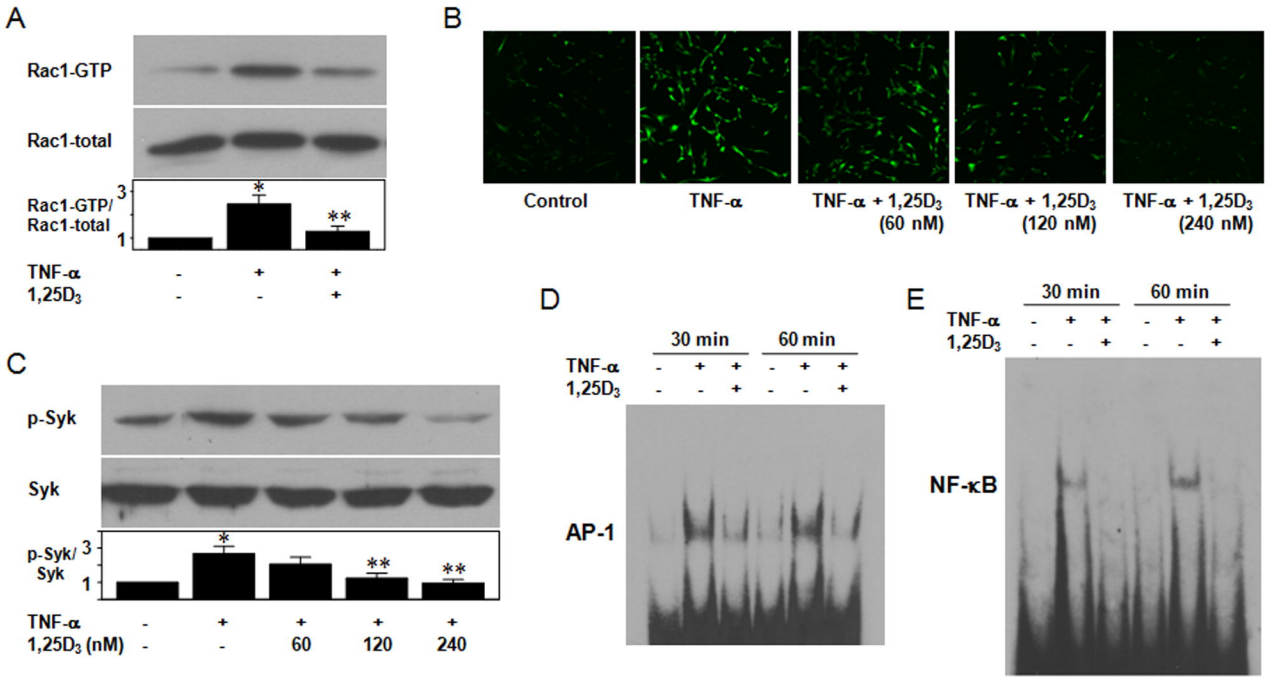
A
Rac1-GTP
Rac1-total
Rac1-GTP/
Rac1-total
3
1
*
**
TNF-α - + +
1,25D3 - - +
B
Control
TNF-α
TNF-α + 1,25D3
(60 nM)
TNF-α + 1,25D3
(120 nM)
TNF-α + 1,25D3
(240 nM)
C
p-Syk
Syk
p-Syk/
Syk
3
1
*
**
**
TNF-α - + + + +
1,25D3 (nM) - - 60 120 240
D
30 min
60 min
TNF-α - + + - + +
1,25D3 - - + - - +
AP-1
E
30 min
60 min
TNF-α - + + - + +
1,25D3 - - + - - +
NF-κB

Figure 5

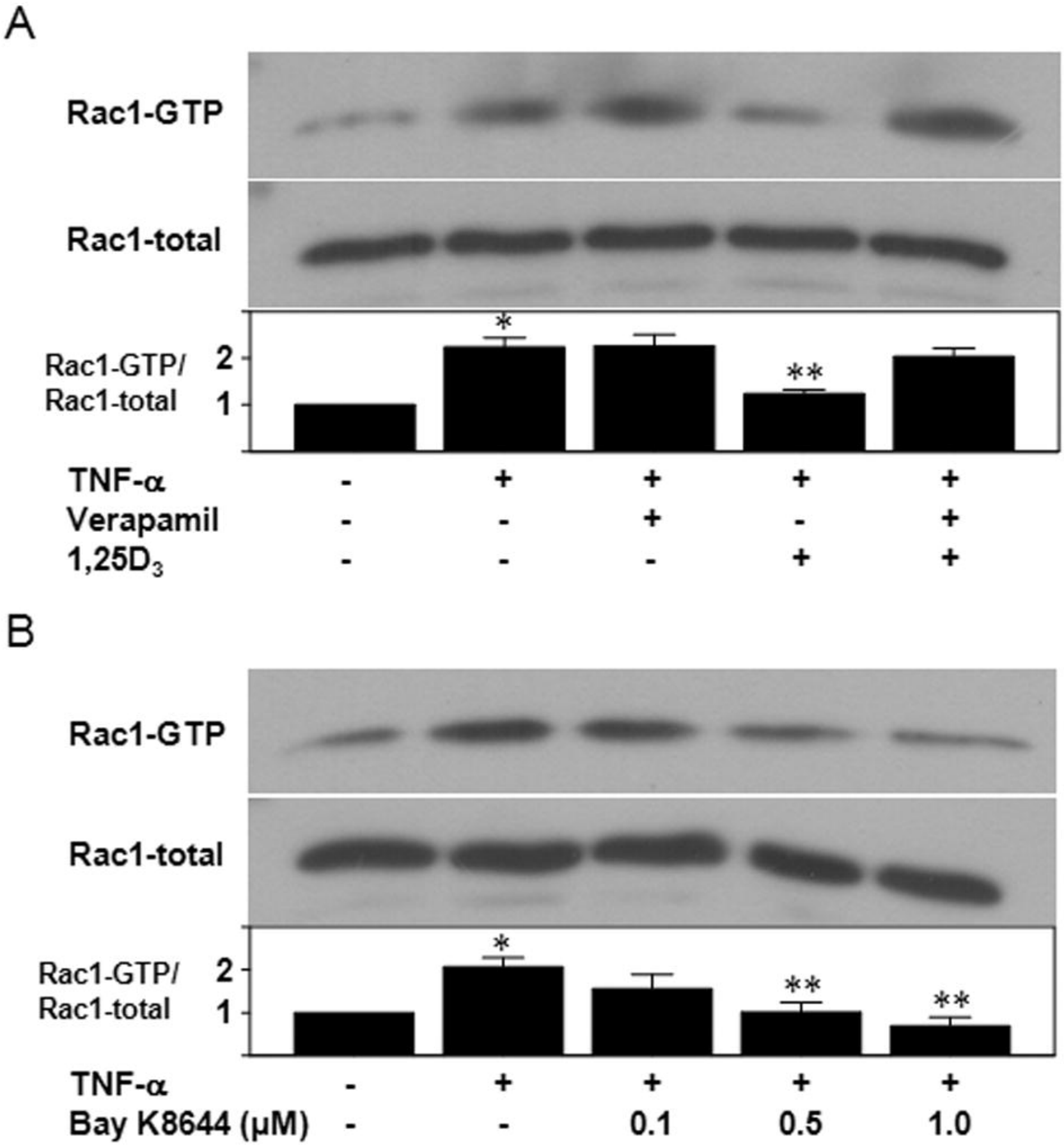
A
Rac1-GTP
Rac1-total
Rac1-GTP/
Rac1-total
2
1
*
**
TNF-α
Verapamil
1,25D3
B
Rac1-GTP
Rac1-total
Rac1-GTP/
Rac1-total
2
1
*
**
**
TNF-α
Bay K8644 (μM)
0.1
0.5
1.0

Figure 6

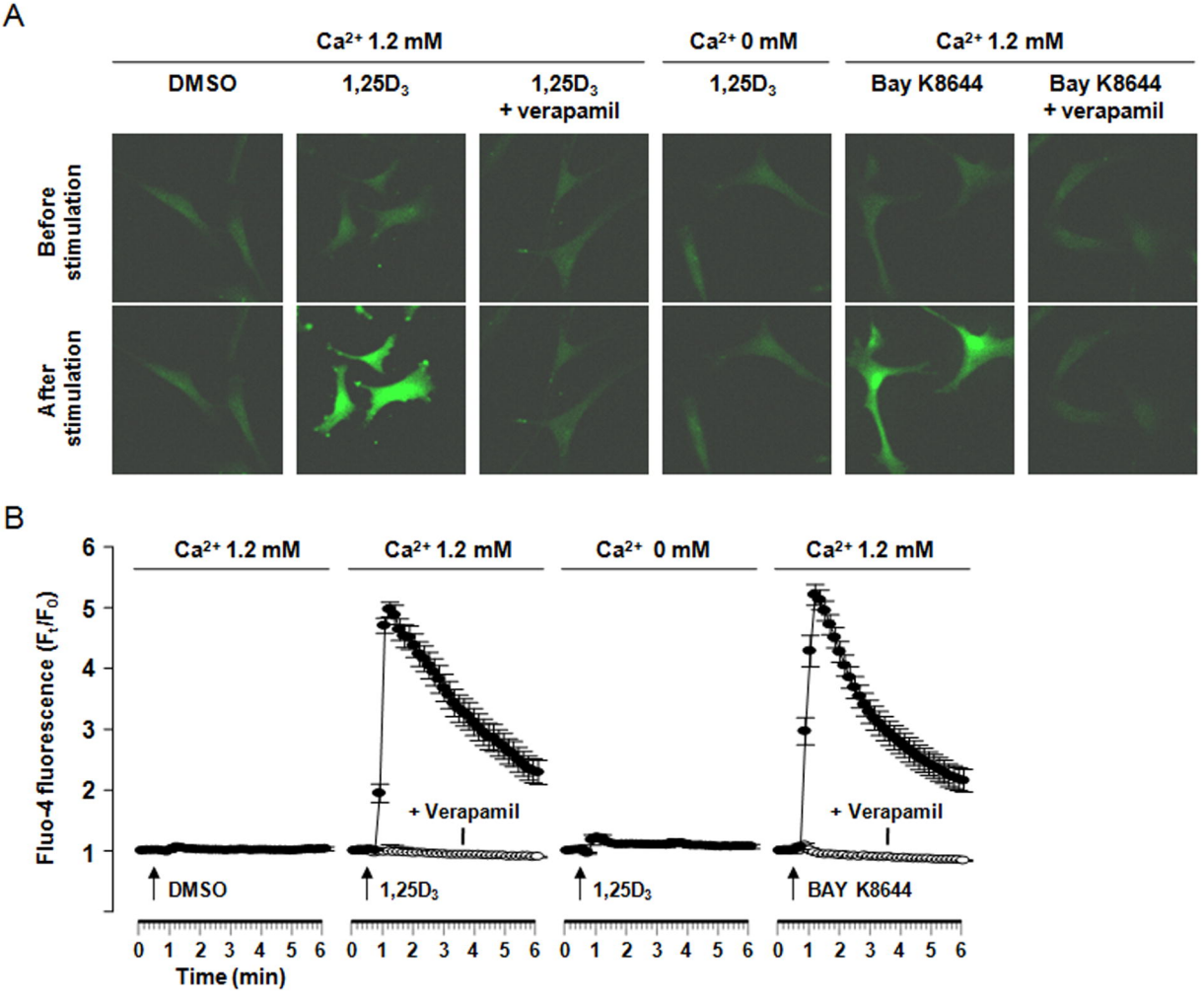
A
Ca2+ 1.2 mM
Ca2+ 0 mM
Ca2+ 1.2 mM
DMSO
1,25D3
1,25D3 + verapamil
1,25D3
Bay K8644
Bay K8644 + verapamil
Before stimulation
After stimulation
B
Ca2+ 1.2 mM
Ca2+ 1.2 mM
Ca2+ 0 mM
Ca2+ 1.2 mM
Fluo-4 fluorescence (F1/F0)
+ Verapamil
+ Verapamil
DMSO
1,25D3
1,25D3
BAY K8644
Time (min)

Figure 7

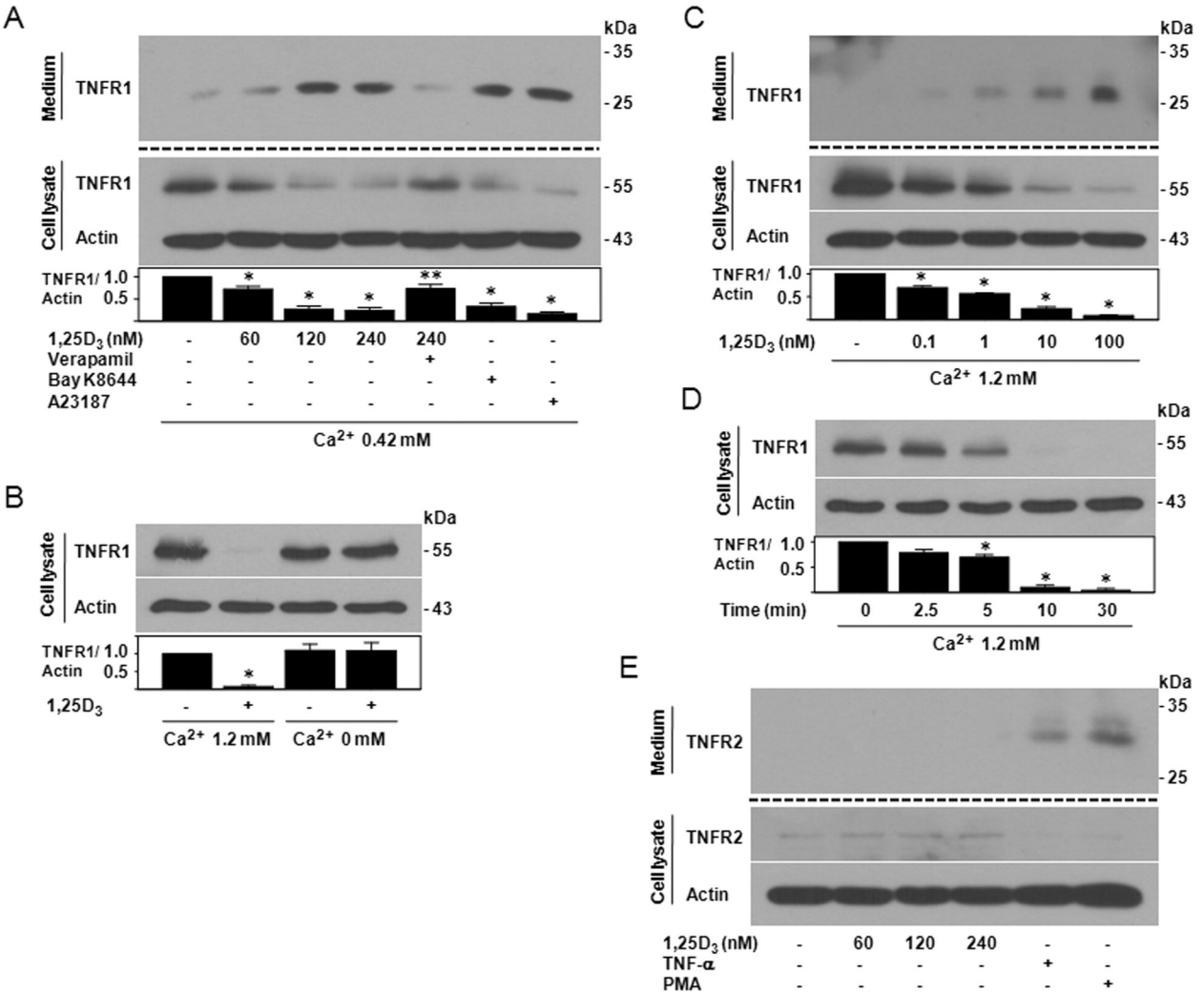
A
kDa
Medium
TNFR1
35
25
Cell lysate
TNFR1
Actin
55
43
TNFR1/ Actin
1.0
0.5
1,25D3 (nM) - 60 120 240 240 - -
Verapamil - - - - + - -
Bay K8644 - - - - - + -
A23187 - - - - - - +
Ca2+ 0.42 mM
B
kDa
Cell lysate
TNFR1
Actin
55
43
TNFR1/ Actin
1.0
0.5
1,25D3 - + - +
Ca2+ 1.2 mM
Ca2+ 0 mM
C
kDa
Medium
TNFR1
35
25
Cell lysate
TNFR1
Actin
55
43
TNFR1/ Actin
1.0
0.5
1,25D3 (nM) - 0.1 1 10 100
Ca2+ 1.2 mM
D
kDa
Cell lysate
TNFR1
Actin
55
43
TNFR1/ Actin
1.0
0.5
Time (min) 0 2.5 5 10 30
Ca2+ 1.2 mM
E
kDa
Medium
TNFR2
35
25
Cell lysate
TNFR2
Actin
1,25D3 (nM) - 60 120 240 - -
TNF-α - - - - + -
PMA - - - - - +

Figure 8

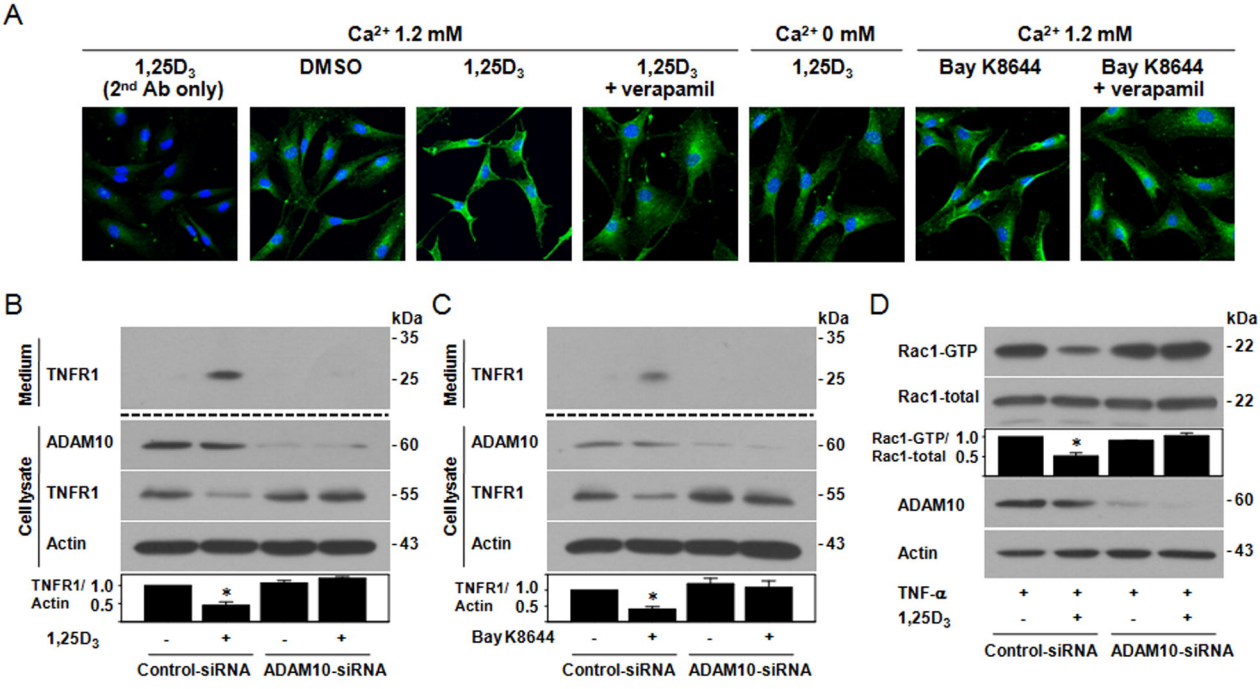
A
Ca2+ 1.2 mM
Ca2+ 0 mM
Ca2+ 1.2 mM
1,25D3 (2nd Ab only)
DMSO
1,25D3
1,25D3 + verapamil
1,25D3
Bay K8644
Bay K8644 + verapamil
B
C
D
kDa
Medium
TNFR1
Cell lysate
ADAM10
TNFR1
Actin
35
25
60
55
43
TNFR1/ Actin
1.0
0.5
1,25D3
Bay K8644
Control-siRNA
ADAM10-siRNA
Rac1-GTP
Rac1-total
22
Rac1-GTP/ Rac1-total
TNF-α